FIRST ANNUAL REPORT

(December 1, 1959 to November 31, 1960)

GRANT NsG 56-60

From

THE NATIONAL AERONAUTICS AND SPACE ADMINISTRATION

to

THE CALIFORNIA INSTITUTE OF TECHNOLOGY

by

Harrison Brown, Principal Investigator

Bruce C. Murray, Associate Principal Investigator

January 31, 1961

Pasadena, California

PART II - SUMMARY OF RESEARCH

CONTENTS OF PART II

1. INTRODUCTION

This is a report of the research activities carried out during the first year of grant NsG 56-60 from the National Aeronautics and Space Agency to the California Institute of Technology. The grant is for basic research pertaining to the moon and planets. Professor Harrison Brown is the principal investigator and Dr. Bruce C. Murray is the associate principal investigator. Part I summarizes administrative and financial information, whereas the present document is intended to provide our co-workers with an interim description of the research activities with which we are now involved. Publication of final results, in general, will be through the customary formal channels of professional journals.

The full-time research staff supported by the grant began work mostly in the last quarter of the grant year and may be augmented slightly during 1961. In addition to Dr. Murray, the staff includes a geochemist, Walter Nichiporuk and two research assistants, Eleanor Helin and Sandy (Y.M.)Liu. Hugh Millard, Kenneth Watson, and David Roddy are 1/3 time graduate research assistants. Victor Nenow and Curtis Baumann, electronic and mechanical technicians of the Division of Geological Sciences, have contributed on a part-time basis. Dr. Alexander Pogo, an expert on the astronomical literature and an accomplished linguist, serves us in a consultant capacity. During the summer months, Gregory Smith, David Roddy, and Dr. Dale Simpson were employed under the grant. The services of the Spectrographic laboratory under Arthur Chodos and the Chemical laboratory under Dr. Donald Maines have been utilized extensively. Also, we wish to gratefully acknowledge the collaborative efforts of Professor Leon T. Silver and of Michel Duke, a National Science Foundation Fellow.

Other presentations of research during 1960, wholly or partly sponsored by this grant, are:

1. Brown, Harrison, "The Density and Mass Distribution of Meteoritic Bodies in the Neighborhood of the Earth's Orbit", JGR, 65, 6, 1679-1683, June, 1960.

2. Helin, E. K. & B. C. Murray, "The Southern California Fireball of September 12, 1960", 21 September, 1960. (Privately circulated to meteoriticists and satellite tracking agencies).

3. Murray, B. C., & A. B. Lees, "An Invariant Property of Satellite Motion in a Dissipative Medium", Presented at the American Astronomical Society Meetings, 16-18 January, 1961, Dallas, Texas, and to be included in the proceedings of those meetings.

4. Watson, Kenneth, Bruce Murray and Harrison Brown, "On the Possible Presence of Ice on the Moon", accepted by the JGR as a Letter to the Editor, January, 1961.

5. Brown, Harrison, "Frequency of Meteoritic Falls", Presented to the Meteoritical Society Meeting, 1960, University of Southern California, Los Angeles, Calif.

6. Brown, Harrison, "Addendum: The Density and Mass Distribution of Meteoritic Bodies in the Neighborhood of the Earth's Orbit", accepted by the JGR as a Letter to the Editor, January, 1961.

In the following sections, the research dealing with first the moon and then with meteorites will be reviewed separately. A bibliography is presented as section 4.

2. LUNAR INVESTIGATIONS

2.1. INTRODUCTION

The overall objective of the lunar research carried out under the grant is the improved understanding of lunar history and, hence, improved understanding of the history of the earth-moon system. A significant improvement in our understanding of lunar history, however, can only result from vastly increased knowledge of the physics, chemistry, and geology of the moon, and particularly of its surface. Much applicable data can be expected to result from the unmanned instrumented probes to be placed on or near the lunar surface during the 1960's. However, these probes must be preceeded and accompanied by a considerable amount of laboratory and telescopic investigations and theoretical analysis in order for the probe measurements to be of maximum scientific significance. It is with this viewpoint of the interdependence of ground-based and probe-borne observations, and with recognition of the decade-long time scale which now characterizes lunar research, that we have selected our preliminary research topics. In particular, we are developing the following four approaches:

(1) systematic collection and analysis of the diverse literature pertaining to observations and interpretation of lunar phenomena.
(2) careful laboratory investigation of the properties of powders in a hard vacuum with particular emphasis on absorption, scattering, and polarization of visible, and eventually infra-red, electromagnetic radiation.
(3) photoelectric observations of selected small portions of the lunar surface in the visible, and eventually in the infra-red, portion of the spectrum
(4) theoretical analysis of processes governing differentiation, transport, concentration, and escape of elements and compounds on the lunar surface.

In regards to literature searching and translation we have been particularly fortunate to acquire the part-time services of Dr. Alexander Pogo, an expert in the Astronomical literature. He and Mrs. Helin, principally, have already accumulated approximately 400 lunar references mostly pertaining to visible and infra-red radiation. In addition, we have had the following articles translated:

Dollfus, Audouin, "Renewed Search for an Atmosphere in the Vicinity of the Moon", Comptes rendus, Vol. 234, pp. 2046-2049, 1952

Fedorets, V. A., "Photographic Photometry of Lunar Service", Trudy Kharkov Astron. Obs., (Vol. 10, old series) Vol. 2, 49-172, 1952 (same as, Learned Notices Khakov State Univ., Vol. 42, 49-172)

Lyot, Bernard and Dollfus, Audouin, "Search for an Atmosphere in the Vicinity of the Moon", Comptes rendus, Vol. 229, pp. 1277-1280, 1949

Orlova, N. S., "Indicatrix of Scattering for the Lunar Surface", Astronomical Circular pub. by Bureau of Astronomical Communications of the USSR Acad. of Sciences, No. 156, pp. 19-21, Jan. 18, 1955

Sharonov, V., "Color Differences on Lunar Surface", Astronomical Circular pub. by Bureau of Ast. Communications of USSR, No. 166, pp. 9-11, Jan., 1956

Yezerskiy, V. and Fedorets, V., "Photographic Spectrophotometry of the Lunar Surface", Academy of Science (Circular) USSR, No. 159, pp. 18-20, March, 1955

Most of these have not been edited, and are not in finished manuscript form. Ultimately, edited versions will be made generally available. However, we would endeavor to make a limited number of copies available to those of our colleagues whose present research topics warrant such special efforts. In the meantime we are slowly augmenting the reference system and translation program with an information classification, storage, and retrieval system designed for lunar and planetary research. The classification scheme used in this system is shown on the next two pages. It is designed to be compatible with the results of direct lunar investigation in the near future, and to eventually be part of a broader classification scheme applicable to the solar system as a whole rather than just to the earth-moon system. Each topic in the classification has a corresponding hole assigned to it on the margin of the 8" x 10" Keysort hand punch-card filing system. Only pertinent information such as observed data, interpretation, accuracy, calibration technique, etc. are included on the 8" x 10" card. Important diagrams or tables are reproduced on the reverse side. Only about 25 cards have been completed so far, but it is hoped to bring the system up to a useful size during 1961.

The powder vacuum studies are still in a preliminary stage. David T. Roddy, a Caltech graduate student employed under the grant, has developed a penetration testing apparatus in conjunction with Dr. Leonard Jaffe, John Rittenhouse and others at J.P.L. His preliminary results indicate that the initial state of packing of the sample governs the penetration results to such a degree that this parameter must be controlled with great care if reproducible results are to be obtained. The data of Seigel (1960) can be contradicted solely by changing the sample-loading technique. An instrument to measure thermal conductivity of dust in a hard vacuum has also been designed and is being fabricated by J.P.L. An experimental system to measure absorption, scattering, and polarization of visible and infra-red radiation by powdered materials in a hard vacuum has been designed by Murray, Roddy, Nenow, and Baumann and is under development. Also, an experimental A.C. polarimeter of our own design using an ADP crystal is presently under test. Collection, preparation, and petrographic and chemical analysis of all rock samples to be used in our powder vacuum experiments are all being carefully supervised by Prof. Leon T. Silver of the Division of Geological Sciences of Caltech. The next three sections summarize recent observational and analytical investigations pertaining to the lunar surface.

(1) NATURE OF OBSERVED QUANTITY
1. Electromagnetic radiation

(2) SUBDIVISION OF SOLAR SYSTEM
1. Moon

(3) SUBDIVISION OF BODY
1. Surface
2. Atmosphere
3. Interior
4. Undifferentiated

(4) FREQUENCY RANGE
1. Radio
2. Microwave
3. Infra-Red
4. Visible
5. Ultra-Violet
6. X Rays
7. Gamma Rays

(5) WAVE CHARACTERISTICS
1. Emission
2. Reflection (WO source specified)
3. Polarized or unpolarized
4. Line
5. Continuum
6. Solar source
7. Terrestrial source (Radar) — For
8. Celestial source — Reflected
9. Other source (Probe) — Radiation
10. Diffraction and scattering
11. Dispersion — At Moon
12. Refraction
13. Geographic variation
14. Time variation
15. Other

(6) METHOD OF OBSERVATION & INSTRUMENTATION
1. Theory of measurement
2. Lens or mirror
3. Spectrum Divider
4. Polarization analyzer or filter
5. Phase comparator
6. One-dimensional intensity measurement
7. Photographic intensity measurement
8. Visual intensity measurement
9. Signal amplifier
10. Calibration technique
11. Other

(7) DEGREE OF INTERPRETATION

1. Raw data or reduced data
2. Theory or procedure of data reduction
3. Physical interpretation
4. Origin & process interpretation
5. Modelling, math simulation, or physical measurement in laboratory
6. Terrestrial analogy
7. Other

(8) SURFACE AND ATMOSPHERIC PARAMETERS

1. Topography
   a. Maria
   b. Uplands
   c. Craters
   d. Other
2. Structure
3. Size and shape
4. Geographic variation
5. Particle size and sorting and roughness
6. Hardness
7. Temperature
8. Thermal conductivity, capacity, etc.
9. Electrical conductivity and other em parameters
10. Composition
11. Organic material
12. Fluid or sublimate phase on surface
13. Albedo and color index or spectrum
14. Luminescence and flourescence
15. Ambient radiation intensity
16. Pressure (Atmospheric)
17. Ion density (Atmospheric)
18. Time variation
19. Other

2.2 A MODEL OF SOLID-VAPOR PHASE EQUILIBRIA ON THE LUNAR SURFACE

Kenneth Watson, Bruce Murray, and Harrison Brown

It has been recognized for some time that gases escape rapidly from the lunar atmosphere because of the low gravitation and the intense radiation level on the lunar surface (Spitzer 1952, Opik & Singer 1960). It has also been presumed that a high escape rate implies that volatile substances, particularly those of low molecular weight, are not now present significantly on the lunar surface, (Kuiper 1952, Urey 1952, Opik & Singer 1960). We wish to point out that high escape rates alone do not necessarily imply high mass removal rates from the lunar atmosphere. Rather it is the vapor pressure of the volatile substance that governs the mass removal rate of that substance from the lunar atmosphere. In the following, we shall develop a model of stability of volatile substances on the lunar surface based on two observed conditions of that surface: (1) the atmosphere, if any, is very rarefied (Elsmore 1957, Dollfus 1952) and, (2) there are permanently shaded areas with maximum temperatures of the order of 120°K (Pettit and Nicholson 1930, Pettit 1940, Sinton 1960). The model may also have direct applicability to the planet Mercury and some of the other planetary satellites.

Under the high vacuum conditions that prevail on the lunar surface, volatile substances will migrate to and condense on the coldest surfaces. This is because the pressure of a volatile substance in a closed system is determined by the temperature at the coldest point in the system: at least as cold as 120°K, for the model in question. The vapor pressure data for various volatiles substances is presented in Fig. 1. The pressure for the solid phases was extrapolated to low temperatures since the experimental data was of the form $\log p = \frac{A}{T} + B$ (A and B constants). Assuming that no solid phase changes occur at these pressures, linear extrapolation is quite reasonable for our purposes. In the case of ice, this assumption is validated by the work of Bridgeman (1957)

For an isothermal atmosphere and constant gas pressure at the surface (corresponding to the vapor pressure) we can calculate the mass of the atmosphere per unit area of the lunar surface as follows. From the Gas Law:

$$\rho = p/RT$$

ρ - density in moles / atmosphere column
p - vapor pressure
R - gas const.

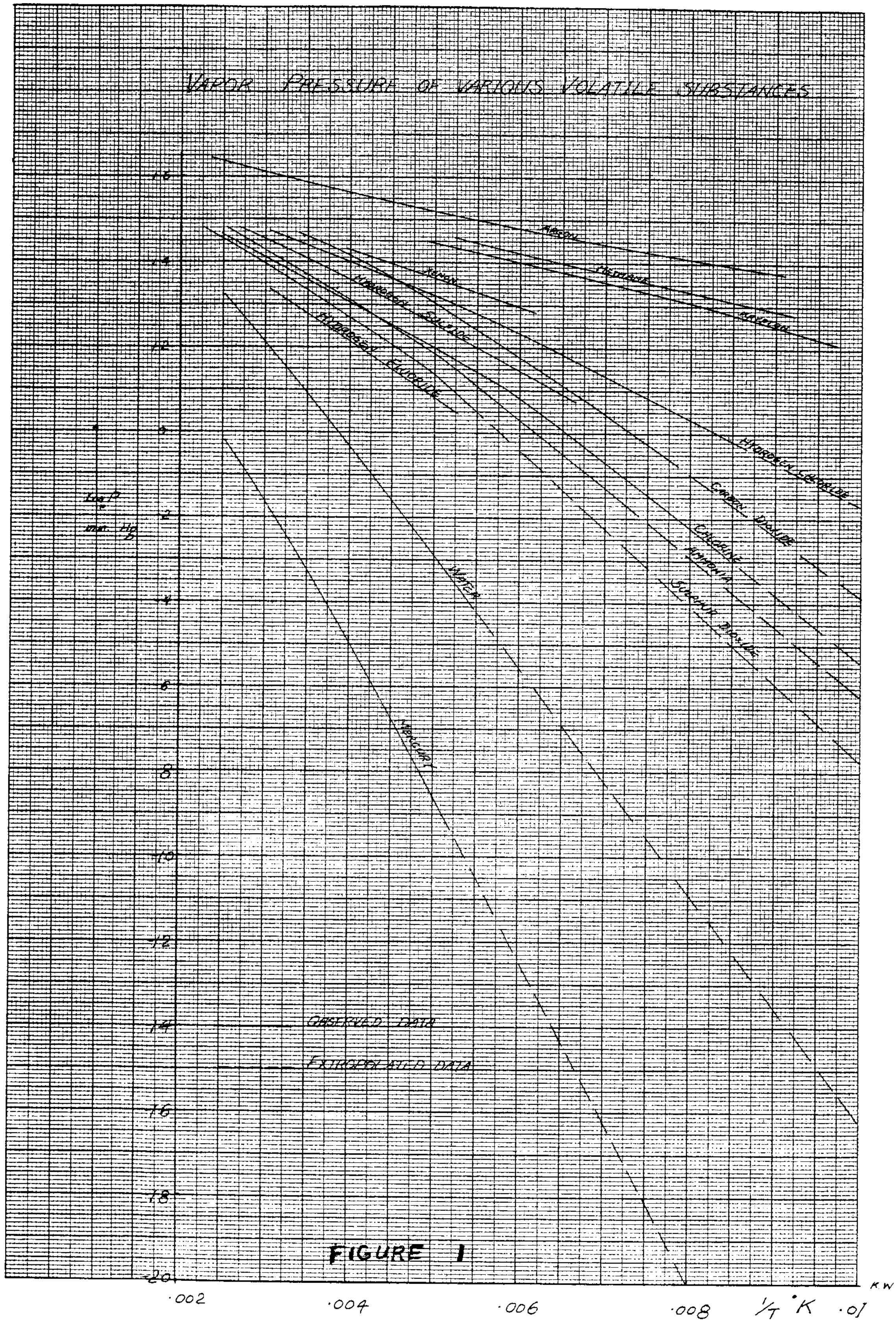
VAPOR PRESSURE OF VARIOUS VOLATILE SUBSTANCES
ARGON
METHANE
XENON
KRYPTON
HYDROGEN SULFIDE
HYDROGEN FLUORIDE
HYDROGEN CHLORIDE
CARBON DIOXIDE
CHLORINE
AMMONIA
SULPHUR DIOXIDE
WATER
MERCURY
OBSERVED DATA
EXTRAPOLATED DATA
Log P mm. Hg
.002
.004
.006
.008
1/T °K
.01

FIGURE 1

T = atmosphere temp. in ^{o}K

Scale height $H_s = \frac{RT}{\mu g}$ from Kinetic theory.

Hence, the mass of atmosphere per unit surface area is:

$$M = \frac{p}{RT}\left(\frac{RT}{\mu g}\right)\mu = \frac{p}{g}$$

and hence, is independent of both temperature and molecular weight.

It follows, then, that the mass loss of any substance in the lunar atmosphere, due to any mechanism is:

$$\dot{m} = \frac{p}{g\tau} \quad \text{in units of mass/area/time}$$

where:

p = Vapor pressure corresponding to coldest point in system
g = surface gravity
τ = relaxation time of escape mechanism.

The least rapid escape rate of volatiles imaginable would be that derived from Kinetic theory assuming direct escape of the fraction of the molecules in the atmosphere which possess velocities greater than the escape velocity. For an isothermal atmosphere at temperature $T^{o}K$ (Spitzer 1952)

$$t_1 = \frac{\sqrt{6\pi}\ C}{3g} \quad \frac{\lambda^{Y}}{Y} \quad \text{where } Y = \frac{3V^2_{\infty_c}}{2C^2}$$

t_1 = relaxation time

C = root mean square velocity $= \sqrt{3Rn}$
$n = T/\mu$
R – gas constant
T – temp. ^{o}K
μ – Molecular wt.

g = gravitational acceleration at lunar surface

V_{∞_c} = lunar escape velocity

$$t_1 = .408 n^{3/2}\ \lambda^{346/n}$$

Results are tabulated (Table One) for various substances at several effective atmospheric temperatures.

TABLE ONE

Gravitational Escape from Lunar Atmosphere

Substance	$t_{\frac{1}{2}}$ 400°K secs.	$t_{\frac{1}{2}}$ 1500°K secs.	$t_{\frac{1}{2}}$ 3000°K secs.
Mercury	2.63×10^{75}	8.53×10^{20}	2.64×10^{11}
Krypton	1.29×10^{32}	7.67×10^{9}	1.38×10^{6}
Chlorine	2.37×10^{27}	5.04×10^{8}	4.00×10^{5}
Sulfur Dioxide	7.44×10^{24}	1.21×10^{8}	2.11×10^{5}
Carbon Dioxide	3.81×10^{17}	2.08×10^{6}	3.67×10^{4}
Hydrogen Chloride	7.44×10^{14}	4.81×10^{5}	2.04×10^{4}
Water	2.47×10^{8}	1.97×10^{4}	7.01×10^{3}
Ammonia	1.16×10^{8}	1.71×10^{4}	6.78×10^{3}

$g = 162$ cms/sec^2
$R = 8.317 \times 10^7$ ergs/°C/mole
$V_\infty = 2.4 \times 10^5$ cms/sec

It is important to realize that no matter how small τ might be imagined, $\dot{m}$ physically cannot exceed the evaporation rate of the substance in question. Hence for the important case of maximum removal rate,

$\dot{m} \leqslant \dot{E}K$

$\dot{E}$ = evaporation rate

K = shaded fraction

The maximum rate of evaporation of a substance from the solid or liquid state would occur if the vapor was removed as fast as it formed, so as to eliminate condensation. Now since evaporation and condensation rates are equal when the vapor is saturated, the kinetic theory of condensation can be used to determine the maximum rate of evaporation. From Loeb (1927) the mass loss can be expressed as follows:

$$\dot{\mathcal{E}} = p\sqrt{\frac{\mu}{2\pi RT}} = 4.374 \times 10^{-5}\ p\sqrt{\frac{\mu}{T}}$$

where,

$\dot{\mathcal{E}}$ = mass loss in gms/cm^2/sec

p = vapor pressure in dynes/cm^2

μ = molecular weight

T = absolute temperature

Table 2 lists the evaporation rates of various volatile substances.

TABLE TWO

Substance	Evaporation Rates at 120°K gms/cm²/sec	gms/cm²/million years
Mercury	3.07×10^{-22}	9.70×10^{-9}
Water	3.12×10^{-14}	9.85×10^{-1}
Sulfur Dioxide	4.25×10^{-7}	1.34×10^{7}
Ammonia	5.69×10^{-6}	1.80×10^{8}
Chlorine	7.12×10^{-5}	2.25×10^{9}
Carbon Dioxide	1.11×10^{-3}	3.50×10^{10}
Hydrogen Chloride	2.66×10^{-2}	8.39×10^{11}
Krypton	3.05×10^{1}	9.62×10^{14}

Summarizing briefly, we have shown that the mass loss of any volatile substance for a variety of mechanisms is determined by the relaxation time for the process and the vapor pressure of the substance at the coldest temperature. Irrespective of these mechanisms however, the escape rate cannot exceed the evaporation rate. Table Two clearly illustrates that water and mercury have low enough evaporation rates at 120°, to remain in the solid phase in appreciable amounts over millions of years.

We can estimate an upper limit for K (shaded fraction) by assuming that as much as 50 percent of the lunar surface is shaded ($K = \frac{1}{2}$). The actual area of permanent shading is considerably less, and for our purposes it will be sufficient to use $K = 10^{-4}$ (Watson et al. 1961). Table Three presents these results.

TABLE THREE

SUBSTANCE	EVAPORATION LOSS FROM ENTIRE LUNAR SURFACE gms / years	gms / 10^9 years
Mercury	3.68×10^{-1}	3.68×10^{8}
Water	3.74×10^{7}	3.74×10^{16}
Sulfur Dioxide	5.09×10^{14}	5.09×10^{23}
Ammonia	6.83×10^{15}	6.83×10^{24}
Chlorine	8.54×10^{16}	8.54×10^{25}
Carbon Dioxide	1.33×10^{18}	1.33×10^{27}
Hydrogen Chloride	3.18×10^{19}	3.18×10^{28}
Krypton	3.65×10^{22}	3.65×10^{31}

As a result of meteorite falls, volatiles are probably liberated from the lunar surface. The fraction which will be retained in the permanently shaded areas will depend upon relative rates of the molecular transport to the poles and the escape.

2.3 PHOTOELECTRIC STUDY OF A SUSPECTED COLOR VARIATION IN MARE SERENITATIS

Bruce Murray & S. Liu

Photographs of Mare Serenitatis clearly demonstrate the existance of a uniform difference in color and/or reflectivity between the surface materials of the central and marginal areas. The present investigation was designed to test the hypothesis that this observable difference in density on the photographs is due, in part at least, to a difference in spectral distribution of intensity, i.e., to a difference in color between the central and marginal areas. No such difference was detected and these results appear to be at variance with those of Keenan (1931).

The Cassegrain scanner of the 60" reflector at Mt. Wilson was used on the night of 3-4 December, 1960 to obtain spectra from 3900 Å to 8100 Å from four small areas in Mare Serenitatis. Each area was observed twice with a blue filter using the second order of the grating and twice with a yellow filter using the first order, resulting in sixteen profiles for comparison. The slit-width was 8" x 8", equivalent to an area 15 km x 15 km on the lunar surface. The slit position, referenced to local lunar features, was also recorded photographically once per minute as a check on the actual position of the slit during each scan. The two areas in the darker, marginal region are located:

(1) immediately northeast of Menelaus, $\lambda = 24^{\circ}40'$, $\beta = 29^{\circ}40'$
(3) in the center of the bay Le Monnier, $\lambda = 45^{\circ}30'$, $\beta = 45^{\circ}10'$

the two areas in the lighter, central region are located:

(2) southeast of Bessel and due north of Menelaus, $\lambda = 26^{\circ}0'$, $\beta = 36^{\circ}0'$
(4) due east of Le Monnier and north northwest of Bessel, $\lambda = 35^{\circ}40'$, $\beta = 40^{\circ}10'$

The numbers (1), (2), (3), (4) are used in Tables I and II also to identify the locations.

The exit slit of the scanner was set at 0.8 mm, corresponding to 8 Å in the second order and 16 Å in the first order. The time constant was 1 second and the scanning rate 200 Å / min. Calibration of wavelength was accomplished by observing a standard reference star (Oke, 1960) before and after the lunar observations. Inasmuch as the transparency of the atmosphere showed a moderately large change between calibrations, and some noise is evident on the calibration runs, no attempt has been made to determine either relative or absolute brightness of the four selected locations.

The overall wavelength range 3900-8100 Å was subdivided into 13 intervals to facilitate the color comparison. The boundaries of the intervals correspond to prominent absorption features in the lunar spectrum when measured with a 8 Å or 16 Å bandpass. Each interval was planimetered and the % total area of that profile computed. This quantity is referred to as % total response in the Tables. The mean value of each pair of runs for each of the thirteen intervals is shown on Table I, along with the estimated standard deviation (computed as half the difference between the two repeated runs). σ is, thus, a measure of the random error involved in returning to the exact location on the lunar surface, as well as that resulting from equipment and atmospheric noise, and from data reduction, particularly that introduced by planimetering. It is clear from Table I that such sources of random error have introduced a dispersion into the data of just under 0.1%, expressed in the units of Table I. Accordingly, we consider the experiment capable of detecting any differences in total intensity between the thirteen intervals of magnitude greater than about 0.3%. Table II summarizes the variations in spectral distribution of intensity of the four stations. It is clear that deviations between stations 1 and 3 taken together and 2 and 4 taken together do not suggest that there are two distinct populations of lower deviation than that formed by taking all four stations together. Similarly, the last two columns of Table II show that even comparison of individual intervals does not result in differences between the intensities of marginal and central areas which are inconsistent with a basic random error of measurement of 0.1%. Accordingly, we conclude that the surface materials of the marginal areas differ significantly from those in the central areas only in reflectivity.

The absence of color differences may be taken as suggesting that the maria surface is compositionally homogeneous. However, the difference in reflectivity is, nevertheless, real and is not easily explained merely as a difference in physical state of the presumably granular material that forms the surface. In any case, the observable density difference on the photographs demonstrates clearly the existance of an intrinsic difference in the surface deposits and is entirely inconsistent with the possibility of a homogeneous surface layer present over the entire maria.

TABLE I - COLOR COMPARISON DATA

INTERVAL From	To	AREA # 1 % Total Response	σ	AREA # 2 % Total Response	σ	AREA # 3 % Total Response	σ	AREA # 4 % Total Response	σ	$\bar{\sigma}$
Part I - BLUE FILTER (2nd ORDER)										
3907	4095	11.92	0.08	11.95	0.14	11.93	0.015	11.67	0.04	0.07
4095	4313	18.50	0.05	18.45	0.13	18.36	0.075	18.35	0.055	0.075
4313	4538	25.47	0.135	25.61	0.035	25.50	0.14	25.53	0.15	0.115
4538	4713	21.56	0.07	21.59	0.065	21.79	0.08	21.66	0.045	0.065
4713	4870	14.46	0.085	14.29	0.10	14.32	0.06	14.49	0.10	0.09
4870	5029	8.06	0.05	8.07	0.045	8.06	0.005	8.25	0.155	0.05
	Total	99.97%		99.96%		99.96%		99.95%		
	$\bar{\sigma}$		0.08%		0.06%		0.06%		0.08%	0.08%
Part II - YELLOW FILTER (1st ORDER)										
4792	5179	11.17	0.195	10.78	0.065	10.85	0.07	10.64	0.065	0.10
5179	5594	16.11	0.01	15.64	0.005	15.73	0.05	15.45	0.035	0.025
5594	5901	13.22	0.27	13.27	0.105	13.22	0.05	13.22	0.14	0.14
5901	6574	26.79	0.205	27.28	0.165	26.97	0.04	26.95	0.105	0.125
6574	6886	10.31	0.005	10.33	0.07	10.44	0.015	10.51	0.04	0.03
6886	7622	17.04	0.155	17.39	0.15	17.38	0.145	17.77	0.155	0.15
7622	8100	5.30	0.115	5.26	0.07	5.37	0.00	5.40	0.02	0.065
	Total	99.94%		99.95%		99.96%		99.94%		
	$\bar{\sigma}$		0.14%		0.09%		0.05%		0.08%	0.09%

Note: The % total instrument response is the average of two runs.
The standard deviation σ is computed as half the difference between the two runs.

TABLE II

TEST OF COHERENCE OF COLOR DATA

INTERVAL		POPULATION 1,2,3,4 B_{1234}	σ_{1234}	POPULATION 1,3, B_{13}	σ_{13}	POPULATION 2,4 B_{24}	σ_{24}	ΔB	$\frac{\Delta B}{\sigma_{13}+\sigma_{24}}$
3907	4095	11.86	0.08	11.92	0.62	11.81	0.14	0.11	0.69
4095	4313	18.42	0.04	18.43	0.70	18.40	0.05	0.03	0.04
4313	4538	25.52	0.04	25.48	0.15	25.57	0.04	0.09	0.47
4538	4713	21.66	0.06	21.68	0.12	21.64	0.04	0.04	0.25
4713	4870	14.39	0.06	14.39	0.07	14.39	0.10	0.00	0.00
4870	5029	8.11	0.05	8.06	0.00	8.16	0.09	0.10	1.11
		ave.	0.065%	ave.	0.18%	ave.	0.08%	0.07%	
4792	5179	10.86	0.13	11.01	0.16	10.71	0.07	0.30	1.30
5179	5594	15.74	0.16	15.94	0.17	15.54	0.10	0.40	1.48
5594	5901	13.21	0.02	13.22	0.00	13.24	0.02	0.02	1.00
5901	6574	27.00	0.21	26.88	0.09	27.12	0.17	0.24	0.92
6574	6886	10.40	0.05	10.38	0.06	10.42	0.09	0.04	0.27
6886	7622	17.40	0.17	17.21	0.17	17.58	0.19	0.37	1.03
7622	8100	5.34	0.04	5.34	0.04	5.33	0.07	0.01	0.09
		ave.	0.11%	ave.	0.10%	ave.	0.10%	0.20%	

NOTE:

B_{1234} mean of Areas 1,2,3,4

B_{13} mean of Areas 1 and 3

B_{24} mean of Areas 2 and 4

σ_{1234}, σ_{13}, σ_{24} are respective standard deviations.

ΔB = difference in means of (1,3) and (2,4).

$\frac{\Delta B}{\sigma_{13}+\sigma_{24}}$ is a rough test of significance for each interval.

2.4 THE POSSIBLE MINERALOGICAL SIGNIFICANCE OF LUNAR & PLANETARY INFRA-RED RADIATION

Bruce Murray

There are two properties of silicate (and other) minerals which may sufficiently alter the infra-red spectrum of the moon and terrestrial planets to permit some mineralogical information to be obtained by means of ground-based, or satellite-or probe-borne telescopes. The two properties are: (1) absorption - reflection bands and transmission bands related to characteristic vibrations of (SiO_4) tetrahedrons and to electronic transactions, and, (2) endothermic and exothermic phase changes of characteristic magnitudes which take place at specific temperatures during heating or cooling of mineral samples. Both properties have been extensively exploited for laboratory analysis of powdered samples of terrestrial materials. Figure 1 , illustrates why the moon might be considered as an object for both reflection and emission spectroscopy in the infra-red. For wavelengths shorter than about 2.7μ, the reflected solar radiation dominates the total infra-red spectrum, whereas the emitted "black-body" radiation dominates the longer wavelength region. During an eclipse, or near the terminator, one might, in addition, be able to obtain an emission spectrum during the rapid cooling or heating of a portion of the lunar surface. Accordingly three possible spectrographic regimes may be resolved: (1) reflection spectroscopy in the near infra-red out to about 3μ, (2) emission spectroscopy in the interval from about 2.5μ to 15μ , of sunlit or shaded areas which are at constant temperatures,* and, (3) emission spectroscopy in the same wavelength interval during periods of rapid temperature changes on the lunar surface. Case (2) has not yet been adequately investigated in the present study to warrant further discussion here. Cases (1) and (3), however, already indicate some promise. Before proceeding, however, it may be worthwhile to mention why the mineralogical composition as well as the chemical composition of the moon or planets is of paramount interest as a means of learning about the degree of chemical differentiation of such a body.

The silicates exhibit a well-known variation in crystal structure characterized by increased sharing of the oxygen ions of the unit (SiO_4) tetrahedra. A decrease in melting point, density, and (Fe,Mg) content parallel this crystallographic variation. In particular, olivine (Fe,Mg)SiO_4 and quartz SiO_2, common terrestrial minerals, are

---

* This is the case to which Sinton and Strong's (1960) observations of Mars and the Moon belong. It is not clear from that paper why they consider that the absence of silicate absorption bands in their spectra proves the absence of silicates.

representative of the two ends of the series. It may prove particularly important to planetology that the I.R. absorption bands of the silicates also show a regular shift in wavelength corresponding to increased sharing of the oxygen ions, as demonstrated by Launer (1952). Hence, infra-red spectroscopy, if feasible at all, may provide information directly about the degree of chemical differentiation of the lunar and planetary surface materials. Furthermore, quartz and olivine are virtually mutually exclusive in terrestrial mineral assemblages and there is little reason to suppose that this would not also be the case for the moon or terrestrial planets. Hence, any spectrographic technique which might distinguish between quartz and olivine is of particular significance, although determination of intermediate minerals is also important.

Returning to the consideration of Case (1), spectroscopy of reflected radiation shorter than about 3μ, it is of interest to note that quartz shows no significant opacity from the visible up to about 2.7μ. Olivine, on the other hand, has a prominent absorption band at 1μ related to an electronic transition due to the Fe^{++} ion (Clark 1957). There are no important variations in index of refraction - and hence in the reflection coefficient - for either mineral over the interval in question. Therefore, one would expect a reflection minimum at 1μ if olivine is present in appreciable quantities on the surface whereas quartz should not modify the spectrum at all. Furthermore, the same absorption band apparently is present also in iron glasses, i.e., similar to olivine in composition. Both the uniqueness of the 1μ absorption band and the deleterious effects of scattering from a granular aggregate obviously require additional experimental investigation before reflection spectroscopy of the moon, for instance, could be expected to yield meaningful mineralogical information. However, such experimental investigations certainly seem warranted, as also would be the preliminary design of suitable telescope instrumentation.

Similarly distinct absorption bands are present in both crystalline and glassy quartz (9.2μ) and olivine (10.0μ) in the emission range. The 9.2μ band of SiO_2 is virtually unique, in fact. Both bands, fortunately, are well within the I.R. atmosphere window. The absorptions, however, are due to lattice vibrations and coincide with reflection <u>maxima</u> and transmission minima. Accordingly, it is possible that during the rapid cooling associated with an eclipse, for example, the cooler particles of the very top of the lunar surface may introduce a characteristic absorption band in the otherwise "black-body" radiation emanating from the still warm layer immediately beneath (the thickness of such a layer would be perhaps a small fraction of a millimeter). This emission phenomena depends, of course, on the behavior of the emissivity of these substances at wavelengths close to the absorption bands as well as on the scattering mode and, therefore, also needs further experimental investigation. Virtually all rock-forming silicates have some strong and usually diagnostic absorption bands in the useful range for ground-based observations as is shown in figure 2 . Hence, emission spectroscopy might reveal a wealth of mineralogical detail if these absorption bands are impressed - even slightly - on the emitted thermal radiation spectrum during cooling, heating, or even under steady-state temperature conditions.

Endothermic or exothermic phase changes in silicates and other minerals, possibly present in the surface deposits of the moon or terrestrial planets, might be detectable during rapid heating or cooling as irregularities in the observed rate of change of temperature. Such irregularities could arise because the temperature of the mineral holds constant briefly during such a phase change. Inasmuch as these phase changes involves crystallographic rearrangements, however, they are not to be expected in glasses. A more serious limitation is that virtually all the phase changes that occur below 400°K are due to the presence of water of hydration. In the case of the moon at least, hydrated compounds probably would be unstable at the surface, even if they once had formed. Mars, however, might present a more favorable situation for the application of the suggested technique in the vicinity of the terminator.

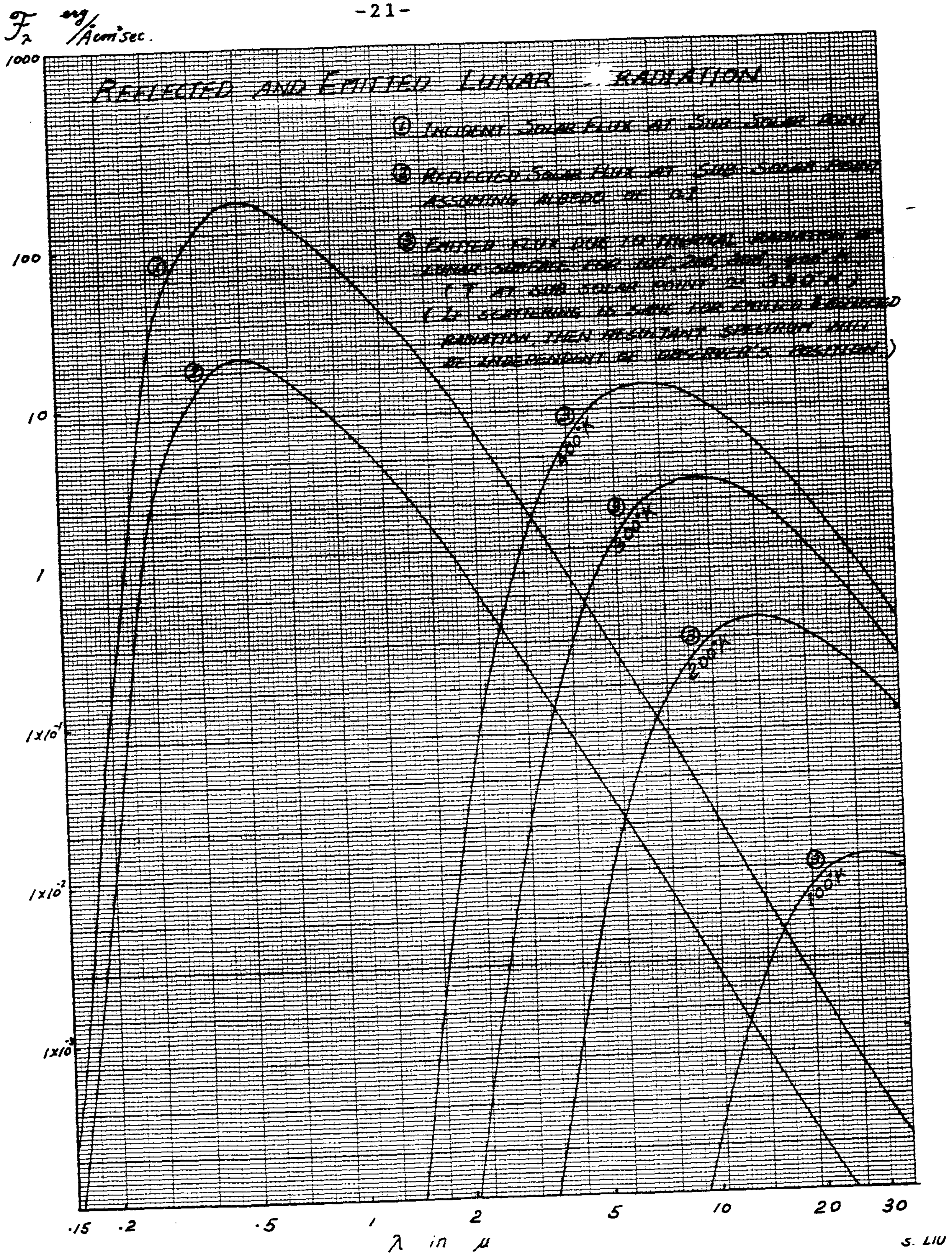
$\mathcal{F}_\lambda$ erg/Å cm² sec.
REFLECTED AND EMITTED LUNAR RADIATION
① INCIDENT SOLAR FLUX AT SUB-SOLAR POINT
② REFLECTED SOLAR FLUX AT SUB-SOLAR POINT ASSUMING ALBEDO OF 0.1
③ EMITTED FLUX DUE TO THERMAL RADIATION OF LUNAR SURFACE FOR 100, 200, 300, 400°K. (T AT SUB SOLAR POINT ≃ 350°K)
(IF SCATTERING IS SAME FOR EMITTED & REFLECTED RADIATION, THEN RESULTANT SPECTRUM WILL BE INDEPENDENT OF OBSERVER'S POSITION.)
1000
100
10
1
1x10⁻¹
1x10⁻²
1x10⁻³
400°K
300°K
200°K
100°K
.15
.2
.5
1
2
5
10
20
30
λ in μ
S. LIU

STRONG INFRARED ABSORPTION BANDS OF SILICATES

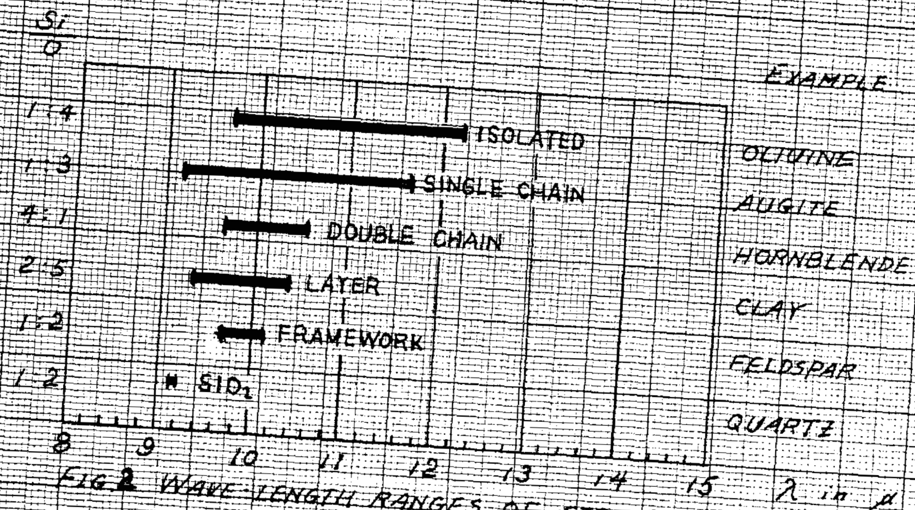

FIG 2 WAVE-LENGTH RANGES OF STRONG INFRARED ABSORPTION BANDS OF SILICON-OXYGEN GROUPS. AFTER LAUNER (1952)

3. METEORITE INVESTIGATIONS

3.1 INTRODUCTION

From at least two points of view, an understanding of meteorites is related to an understanding of the moon. There are probably compositional relationships between the two. Further, meteorites undoubtedly strike the moon with sufficient frequency to have had major effect upon lunar topography. In view of the importance of meteorites in relation to lunar research, a significant fraction of the effort connected with this grant has been placed upon meteoritic research.

The first area of inquiry has involved meteorite systematics. The data contained in the "Catalogue of Meteorites" by G. T. Prior and M. H. Hey (1953 edition) has been placed on IBM punch cards together with supplementary data provided by the bulletins of E. L. Krinov, under the auspices of the International Geological Congress. These cards have been used to compile listings of meteorites based upon chronology, type of meteorite, and geographical position. An additional benefit has been the modernization of tabulations showing the numbers of meteorite falls as functions of the time of day, month, year, geographical position and type of meteorite. Summaries of these listings will be made available in the near future.

Studies have been made of the chemical composition of meteorites using convential chemical techniques as well as X-ray fluorescence. In the study of the Bruederheim Meteorite the chemical analysis has been correlated with petrographic studies. The X-ray studies have been conducted with particular reference to the applicability of X-ray fluorescence analysis to the determination of the chemical composition of the lunar surface.

A preliminary study has been made by Mr. David Roddy of the applicability of differential thermal analysis to meteorites. The results made it appear likely that this type of analysis can provide useful information concerning the phase composition of meteorites.

3.2 METEORITE STATISTICS

Harrison Brown and Hugh T. Millard, Jr.

The available data on meteorites summarized in sources such as the Prior - Hey catalogue have been placed upon punch cards, and these cards have been sorted through with respect to specific variables. Each meteorite has been assigned a code number and the punched data includes, when available, the time and date of the fall, the location (rounded to one degree), the type of meteorite, the recovered mass, the number of fragments, together with chemical data such as the per cent of nickeliferous iron, the Fe/Ni ratio in the metal, the MgO/FeO ratio in the silicate phase, the per cent nickel and the per cent troilite.

Printouts have been obtained of the data with respect to a number of variables. The following printouts are now available:

1.) all meteorites in alphabetical order
2.) falls in chronological order
3.) falls by month and day
4.) falls by hour, local time
5.) iron falls by type
6.) iron falls by mass
7.) stony-iron falls by type
8.) chondritic falls by type
9.) achondritic falls by type
10.) chondritic falls by weight
11.) achondritic falls by weight
12.) meteorites in each interval of 10° latitude in longitudinal order
13.) meteorites in each latitude interval by month
14.) meteorites in each latitude interval by time of day
15.) falls in order of metal phase content
16.) iron finds by type
17.) iron finds by weight
18.) stony-iron finds by type
19.) stony finds by weight
20.) stony finds by type
21.) finds by latitude and longitude
22.) finds in order of metal phase content
23.) iron meteorites in order of increasing nickel content.

These data are now being analysed and plotted for distribution.

Geographical locations of falls and finds have been plotted on maps for the purpose of analysing the flux of meteorite falls upon the earth. An estimate of the frequency of impact of meteorites upon the earth and moon has been made, based upon the observed impact frequency in areas of high population density. It appears that the flux of meteorites reaching the earth's surface corresponds to about 1.1 meteorites per year per million square kilometers.

Analysis of the fall data indicates that certain types of meteorites fall preferentially during specific times of the year. For example, veined white hypersthene chondrites appear to fall preferentially in February, May and September. There are distinct groupings of iron meteorite falls in the intervals March 25-April 20 and July 7-August 3. Among the hypersthene chondrites there are interesting groups of falls which appear to cluster around June 28, July 18, September 5 and December 10, which may relate to orbital characteristics of individual meteorite groups. By contrast, falls of carbonaceous chondrites appear to be randomly distributed throughout the year.

The summaries of these studies will be made generally available soon.

3.3 THE PETROGRAPHY OF THE BRUEDERHEIM METEORITE

Dale R. Simpson

The Bruederheim Meteorite fell in 1960 and has been used extensively by other workers in studies of spallation reactions induced by cosmic rays. In view of the fact that so many workers are studying this meteorite, it was deemed desirable to make a careful petrographic study of the meteorite together with a careful chemical analysis. The description below is preliminary. An independent opinion of many of these observations, based upon his own study of the thin and polished sections, is being prepared by Mr. Michael Duke.

PETROGRAPHY

Texture

The meteorite is holocrystalline inequigranular. Chondrules, spherical to subspherical minerals or mineral aggregates, form the most conspicuous textural features. The chondrules are in a fine to medium crystalline groundmass. This groundmass is seriate textured with the smallest grains being about 0.01 mm. in diameter. The larger grains of the groundmass are as much as 0.3 mm. in diameter. They are generally anhedral and have forms that range from angular to subrounded.

In this study, the chondrules have been divided into seven classes on the basis of their morphology. The names assigned to these classes are intended to be descriptive and not genetic and for this reason the use of a mineral name in the name of a chondrule class has been avoided wherever possible. The descriptive names are the following:

1. Rimmed bar chondrules
2. Radial aggregate chondrules
3. Lathlike aggregate chondrules
4. Composite acicular chondrules
5. Composite equant olivine chondrules
6. Equant olivine chondrules
7. Single crystal chondrules

It should be understood that there are many chondrules in this meteorite that do not fit well into a single class; in fact there appear to be gradations between some of the classes. Therefore the chondrules described and the class names assigned should be considered textural end-members.

1. Rimmed bar chondrules. Two such chondrules were observed in the thin section, each about 0.6 mm. in diameter. The core of these chondrules, about 0.5 mm. in diameter contains elongate anhedral crystals of olivine in subparallel orientation with the individual crystals extending across the chondrule core. There are about 10 of these elongate olivine crystals in crude optical continuity with each other in a single chondrule. In one of these, the olivine has $2V = +85^{\circ}$ corresponds to $Mg85Fe15$. An average width of these olivine crystals is about 0.02 mm. Interstitial to the elongate olivine crystals is pyroxene. This interstitial mineral may be a single crystal or more crystals with a common orientation. In thin section the core of the chondrule appears round and is surrounded by a rim of olivine. There are about 15 crystals in a crude optical orientation with each other in this rim, and in all cases these crystals extend from the core-rim contact to the outer edge of the chondrule. In one of the chondrules the olivine in the core is in optical continuity with the olivine in the rim whereas in the other chondrule there is a marked difference in the optical orientation of the core and the rim. The outer edge of the chondrule appears generally rounded but in detail it is very irregular in outline. Small masses of iron and troilite are present in both the rim and the core of the chondrules.

2. Radial aggregate chondrules. Three exceptionally well developed chondrules of this type were found in the thin section, each about 1.5 mm. in diameter. These chondrules are composed of acicular crystals of pyroxene, the larger of which measure as much as 2 mm. in length and 0.02 mm. in width. In some chondrules these crystals appear to radiate from a common point and thus have a fan-like texture. In other chondrules the acicular crystals are subparallel; whereas in still other chondrules there appear to be domains and in each domain the acicular crystals have a different orientation. Besides the acicular crystals of pyroxene there are rarely present anhedral masses of pyroxene that appear to grade into the acicular crystal form. These anhedral masses of pyroxene, the largest being about 0.3 mm. long, have the same optical properties and orientation as the acicular crystals of pyroxene. Masses of iron and troilite, about 0.02 mm. in diameter are distributed in these radial aggregate chondrules. These chondrules are subrounded with an irregular boundary.

3. Lathlike aggregate chondrules. About 6 to 8 of these chondrules were found in the thin section each about 1 to 2 mm. in diameter. They contain pyroxene with a lathlike habit. These lathlike crystals range in length from about 0.2 to 0.6 mm. and in width from 0.03 to 0.05 mm. An area in a chondrule may be in different optical orientation with another area of the same chondrule,

and within a single area the pyroxene laths commonly have several directions of elongation but a common optical orientation. As a result of the pyroxene laths, the chondrule has a crisscross texture. The laths are nearly adjacent to each other but have a wide-appearing contact as a result of minerals with an equant form in the contact zone. These equant minerals are either isotropic or very low birefringent with relief about equal to the pyroxene. These crystals are about 0.003 mm. in diameter. The outer edge of some of these chondrules is distinct, being marked by a crude concentric fracture; however others of these chondrules do not have a well defined outer edge although the general form of the chondrules is round to subround.

4. Composite acicular chondrules. About 6 to 8 of these chondrules in the thin section average about 1 mm. in diameter. These chondrules are composed of about 50% olivine and 50% pyroxene. The olivine has an acicular habit with individual crystals commonly about 0.3 mm. long and 0.03 mm. wide. These crystals, which are evenly distributed in the chondrule, have a common optical orientation and lie parallel to each other. Interstitial to the acicular olivine crystals are anhedral pyroxene crystals. Some of these pyroxene crystals are as much as 0.08 mm. in diameter. Commonly the anhedral pyroxene crystals are cut by an acicular olivine crystal. Iron and troilite grains, about 0.01 mm. in diameter, are randomly distributed in these chondrules. In general form these chondrules are rounded to subrounded; however some of them appear flattened or broken. Rarely an olivine rim, in optical continuity with the acicular olivine, is present along part of the periphery of the chondrule; however the outer margin of these chondrules is generally irregular and poorly defined.

5. Composite equant olivine chondrules. There are about 4 to 8 in the thin section, each about 1 to 2 mm. in diameter. Olivine, averaging about 0.3 mm. in diameter, comprises about 70% of these chondrules. In some chondrules the olivine forms euhedral crystals with exceptionally well developed faces; however in other chondrules the crystals are subhedral to anhedral and appear embayed or even skeletal. Interstitial and in the embayed areas of the olivine crystals, pyroxene poikilitically encloses numerous olivine crystals that are about 0.007 mm. in diameter. The interstitial pyroxene forms about 30% of the chondrule. Although these chondrules are rounded in form, in detail they have a very irregular border with the limit of the chondrule being defined by the equant olivine crystals.

6. Equant olivine chondrules. There is one good example of this type in the thin section. This chondrule, about 2 mm. in diameter, is composed of small equant crystals near the outer edge and it becomes

coarser crystalline near the center. Most of the crystals near the outer edge of the chondrule are in the size range of 0.02 to 0.07 mm. with an average size of 0.03 mm. These crystals are closely packed with no visible interstitial material. Olivine is the only silicate mineral in the outer portion of the chondrule. The central part is pyroxene poikilitically enclosing olivine. The maximum size of individual pyroxene crystals in the center of the chondrule is difficult to determine because the mineral is extensively fractured; however one pyroxene crystal is at least 0.7 mm. in diameter. An average size of the olivine that is poikilitically enclosed by the pyroxene is about 0.6 mm. in diameter. These olivine crystals are equant and subhedral. Iron and troilite grains as much as 0.1 mm. in diameter are disseminated in the chondrule. In addition, iron, troilite, and wustite occur in a distinct, but discontinuous, band around the chondrule.

7. Single crystal chondrules. There are many examples of this type in the thin section. These single crystal chondrules, commonly about 1 mm. in diameter, may be either olivine or pyroxene. The olivine chondrules are equant, rounded or subrounded, with a well defined outer edge. The pyroxene chondrules are subrounded to subangular also with a well defined outer boundary.

Mineralogy

Metallic Phases

1. Troilite is present in very irregular masses up to about 2 mm. in maximum dimension. These masses appear to fill in or be interstitial to the silicate minerals and in several areas they vein the silicate minerals. These irregular masses are made up of subhedral troilite crystals about 0.1 mm. in diameter.

2. Metallic iron-nickel is present as very irregular masses up to 1 mm. in maximum dimension. It also appears to fill in around the silicate minerals.

3. Wustite occurs as anhedral crystals 0.1 to 0.2 mm. in diameter. In reflected light it appears fractured and pitted.

Non-metallic Phases

1. Pyroxene was identified in several types of chondrules. The optical properties obtained for different mineral fragments are shown in Table 1.

Table I

Optical properties of pyroxenes in mineral fragments of the Bruederheim Meteorite

Occurrence[1]	N [2]	N [2]	Mineral Composition[3]
Radial aggregate chondrule (3)	1.678	1.694	$Mg_{77}Fe_{23}$
Radial aggregate chondrule (4)	1.680	1.692	$Mg_{78}Fe_{22}$
Lathlike aggregate chondrule (8)	1.678	1.690	$Mg_{80}Fe_{20}$
Lathlike aggregate chondrule (11)	1.678	1.690	$Mg_{80}Fe_{20}$
Radial aggregate chondrule (12)	1.678	1.692	$Mg_{78}Fe_{22}$
Lathlike aggregate chondrule (13)	1.677	1.690	$Mg_{80}Fe_{20}$
Single crystal chondrule (15)	1.678	1.690	$Mg_{80}Fe_{20}$

(1) The morphologies of the crystals are listed under types of chondrules.

(2) The indicies of the mineral fragments were obtained in the manner previously described. Because of the size and fragile nature of the mineral fragment it was not possible to orient the specimens on a universal stage, consequently there is uncertainity as to the optical orientation of the mineral fragments. For this reason, the values listed for the indices are considered accurate only to 0.004.

(3) Obtained from diagram of the properties of orthopyroxenes, Hess, H. H., G.S.A. Memoir 80, 1960.

2. Olivine is present in chondrules and in the groundmass. The optical properties obtained for the different mineral fragments are given in Table 2.

Table 2

Optical properties of olivine in mineral fragments of the Bruederheim Meteorite

Occurrance (1)	N (2)	N (2)	N (2)	2V	Mineral Composition (3)
Composite equant - olivine chondrule (5)	1.680	1.700		85°(-)	$Fo_{77}Fa_{23}$
Rimmed bar chondrule (7)		1.690	1.715		$Fo_{77}Fa_{23}$
Equant olivine chondrule (9)	1.678		1.715		$Fo_{77}Fa_{23}$
Composite equant olivine chondrule (10)			1.715		$Fo_{77}Fa_{23}$
Single crystal chondrule (14)			1.715		$Fo_{77}Fa_{23}$
Fine grained groundmass	1.680		1.715		$Fo_{77}Fa_{23}$

(1) The morphologies of the crystals are listed under type of chondrule

(2) The indicies of the mineral fragments were obtained in the manner previously described. Because of the size and fragile nature of the mineral fragment it was not possible to orient the specimens on a universal stage, consequently there is uncertainity as to the optical orientation of the mineral fragments. For this reason, the values listed for the indicies are considered accurate only to 0.004.

(3) Obtained from diagram of properties of olivine, Poldervaart, A., Am. Min., 35, p. 1073, 1950

3. Apatite is present in trace amounts as anhedral crystals interstitial to olivine and pyroxene. Indicies, Nw 1.626 ± 0.002 and $N_{\epsilon} = 1.621 \pm 0.002$ indicate that the mineral is a fluor-apatite.

4. Feldspar was looked for but not found in the thin section.

Modal Analysis of the Metallic Phases

A modal analysis of a polished thin section and a polished section was made in order to determine the per cent iron, troilite, and wustite in the meteorite. The opaque minerals were identified and point counted on a metallographic microscope with a point count stage. With both the polished section and the polished thin section a count of more than 2500 points was made and the values were recorded every 500 points. A plot of per cent mineral vs. number of points, at 500 point intervals, give an indication of the sample area required. Such a plot of this meteorite shows that reproducibility to plus or minus 0.5% of the whole can be expected for the metallic phases from a sample area of about 5 cm^2. In both the polished thin section and the polished section there is about 5% troilite, 3% iron, and 0.5% wustite by volume. Holes present on the surface studied were also counted and it was found that the polished section had more than twice as many holes as the polished thin section. This is probably the result of bonding used to mount the thin section to the glass slide filling the holes. With reflected light the bonding media probably could not be distinguished from the silicate minerals.

Assuming the specific gravity of the pyroxene-olivine mixture to be 3.4, that of wustite to be 5.7, that of troilite to be 4.8 and that of metallic iron-nickel to be 7.8, we find the following composition by weight:

metallic iron-nickel	8.0%
troilite	7.5%
wustite	0.8%
other	83.7%

Thin Section
In volume per cent

Points	Silicates	Wustite	Troilite	Iron	Holes
500	85.8	0.6	7.8	3.0	2.8
1000	85.9	0.4	5.8	3.9	4.0
1500	83.9	0.5	5.3	4.0	4.4
2000	86.3	0.5	5.2	3.7	4.1
2500	86.7	0.6	5.2	3.5	4.0
2665	86.8	0.6	5.3	3.3	3.8

Polished Section

Points	Silicates	Wustite	Troilite	Iron	Holes
500	84.6	0.4	6.0	4.2	4.8
1000	82.4	0.5	5.1	3.9	8.1
1500	82.4	0.7	4.8	3.7	8.4
2000	81.1	0.6	5.1	3.5	9.6
2500	81.0	0.6	5.3	3.3	10.0
2711	81.4	0.5	5.2	3.4	10.0

3.4 CHEMICAL ANALYSIS OF THE BRUEDERHEIM METEORITE

Donald Maynes

Outline of Analytical Methods

From a 60 gm. piece of the meteorite, 15.2 gms. were chipped off and crushed in a Plattner mortar to pass 80 mesh. Those pieces of the metallic phase which flattened into plates during the crushing were reduced to 80 mesh with a Wig-L-Bug.

A second portion of approximately 25 gms. was taken from the same piece, and reduced to 80 mesh. This portion was separated into a "magnetic" and "non-magnetic" fraction with a hand magnet, the weights being 3.1341 and 22.0303 gms. respectively.

Portions of the crushed sample used for the various determinations were separated with a sample-splitter, except that grab-samples were used in the analysis of the "magnetic" fraction.

A 1 gm. portion was used for the determination of H_2O^-, SiO_2, TiO_2, Total Fe, Al_2O_3, CaO, and MgO. H_2O^- was determined from the loss in weight at 105°C. Silica present in the ammonia precipitate was recovered and the weight added to that obtained by double dehydration of an hydrochloric-acid solution. The ammonia precipitate was dissolved and aliquots were taken for the determination of TiO_2 (colorimetrically with hydrogen peroxide), total iron (reduction with silver and titration with potassium dichromate), and Al_2O_3 (gravimetrically by precipitation with 8-hydroxyquinoline). Calcium was precipitated twice as the oxalate, ignited, and weighed as the oxide. Magnesium was precipitated twice with phosphate, ignited, and weighed as the pyrophosphate. Manganese present in the pyrophosphate was determined and the weight of pyrophosphate corrected for its presence. (Hillebrand, Lundell, Bright, and Hoffman, 1953).

Total water was determined by the Penfield method, with lead oxide added to retain other volatile constituents. The value for H_2O^+ was obtained by subtracting H_2O from total water.

Alkalies were determined in a 0.5 gm. sample, essentially in the manner outlined by Brannock and Berthold.(1953).

Manganese and phosphorus were determined in aliquots of a solution of 0.5 gms. of the meteorite; P_2O_5 by the procedure of Kitson and Mellon (1944); MnO by the procedure of Willard and Greathouse (1917).

Total nickel, chromium, and sulphur were determined in a 1 gm. portion after a fusion with a sodium carbonate-potassium nitrate flux. Chromium was determined colorimetrically as the dichromate, sulphur gravimetrically by precipitation with barium chloride, and nickel gravimetrically by precipitation with dimethylglyoxime. (Hillebrand, Lundell, Bright, and Hoffman, op. cit.).

Metallic iron was determined by two methods, namely, Riott's procedure (1941), and the mercuric-chloride procedure (Lundell, Hoffman, Bright, 1931). An aliquot of the solution obtained in the mercuric-chloride procedure was used for the metallic-nickel determination; the insoluble portion of the sample was used for a direct determination of nickel oxide. Generally, Riott's procedure yields the higher result for metallic iron. Experiments with other meteorites have not yet indicated the cause of the difference.

The concentration of iron as oxides, reported as FeO, was obtained by subtracting the sum of metallic iron and iron as sulphide from total iron.

Results

The analytical results are shown in Table I. The average analysis is in satisfactory agreement with the composite result derived from independent analysis of the "magnetic" and "non-magnetic" splits. The chemical results for metallic nickeliferous iron and troilite are compared with the petrographic results below

	Per cent	
	petrographic	chemical
nickeliferous iron	8.0	8.53
troilite	7.5	6.58

The agreement is satisfactory. The discrepancy may in part result from an occasional confusion between metal and troilite under the microscope.

Table I

CHEMICAL COMPOSITION OF THE BRUEDERHEIM METEORITE

	#1	#2	#3	AVERAGE	"magnetic"	"Non-Mag."	"Composite"
SiO_2	39.56	39.54		39.55	15.51	43.31	39.84
TiO_2	0.12	0.12		0.12	0.05	0.12	0.12
Al_2O_3	2.15	2.15		2.15	0.98	2.36	2.19
Met. Fe	($KCuCl_3$) 7.44	($HgCl_2$) 7.18		7.31	53.40	0.36	6.97
$FeO+Fe_2O_3$ as FeO	13.80	13.55		13.89	6.90	14.97	13.87
MnO	0.32	0.32		0.32	Not Determined	0.35	0.31
CaO	1.76	1.79		1.78	0.78	1.94	1.80
MgO	24.66	24.71		24.69	7.77	27.16	24.71
Na_2O	0.99	0.99		0.99	Not Determined	1.07	0.94
K_2O	0.12	0.11		0.12	Not Determined	0.12	0.10
H_2O^+	0.14	0.17		0.16	Not Determined	0.18	0.16
H_2O^-	0.05	0.03		0.04	0.04	0.01	0.01
P_2O_5	0.28	0.27		0.28	Not Determined	0.30	0.26
FeS	6.56	6.59		6.58	2.21	7.25	6.63
TOT. Ni. as metal	1.22	(1.39)(1)	1.22	1.22	9.36	0.12	1.28
Cr_2O_3	0.53	Not (2) Determined		0.53	0.27	0.58	0.54
TOTAL	99.70	99.44(2)		99.73	97.27	100.16	99.73
Tot. Fe as metal	22.35	(21.90)1	22.23	22.29	60.16	16.62	22.04

(1) Discarded in ave.
(2) Cr_2O_3 from Brued. #1 is used.

3.5 MISCELLANEOUS ANALYSES OF METEORITES

Donald Maynes

Several meteorites have been analyzed with respect to their major constituents. The results are summarized in the attached table.

MISCELLANEOUS METEORITE ANALYSES FROM
SILICATE ANALYSIS LABORATORY

	Modoc	Forest City	McKinney	Alamogordo	La Lande	Pantar	Seibert	Cavour	Ladder Creek	Melrose	Ransom
SiO_2	39.90	37.25	39.63	34.77	38.73	37.72	34.79	35.55	38.50	39.00	35.96
TiO_2	0.12	0.11	0.11	0.09	0.11	0.11	0.10	0.10	0.11	0.11	0.11
Al_2O_3	2.04	2.21	2.04	2.00	2.23	2.14	1.97	2.00	2.08	2.17	2.04
Fe Metal	6.42	8.43	5.15	10.64	0.43	15.12	4.98	12.83	1.06	2.38	9.28
FeO Fe_2O_3 as FeO	14.04	14.45	15.61	18.38	22.95	9.34	21.83	13.25	20.16	18.51	16.16
MnO	0.32	0.30	0.31	0.29	0.32	0.31	0.28	0.28	0.31	0.31	0.28
CaO	1.66	1.45	1.72	1.49	1.58	1.81	1.44	1.61	1.79	1.58	1.49
MgO	24.83	23.40	24.86	23.08	23.70	24.82	22.47	22.58	23.77	23.55	22.57
Na_2O	0.97	0.83	0.92	0.62	0.81	0.86	0.66	0.72	0.92	0.77	0.69
K_2O	0.12	0.10	0.11	0.09	0.09	0.12	0.09	0.09	0.11	0.09	0.11
H_2O^+	0.29	1.60	0.49	1.31	2.15	0.43	2.15	1.67	1.70	1.71	1.72
H_2O^-	0.07	0.37	0.07	0.45	0.34	0.11	0.36	0.39	0.18	0.40	0.35
P_2O_5	0.26	0.31	0.27	0.31	0.28	0.33	0.33	0.32	0.26	0.32	0.32
FeS	6.78	5.38	6.84	5.46	3.53	5.19	4.93	5.40	5.85	5.27	5.40
Tot Ni as metal	1.28	1.62	1.14	1.65	1.01	1.76	1.39	1.71	1.06	1.19	1.62
Cr_2O_3	0.54	0.47	0.55	0.51	0.50	0.53	0.47	0.53	0.54	0.55	0.52
TOTAL	99.64	98.28	99.82	101.14	98.40	100.70	98.24	99.03	98.40	97.91	98.62
Tot. Fe as metal	21.56	23.09	21.63	28.40	20.51	25.68	25.08	26.56	20.44	20.12	25.27

MISCELLANEOUS METEORITE ANALYSES FROM
SILICATE ANALYSIS LABORATORY

	Arriba	Hugoton	Coldwater	Covert
SiO_2	38.36	33.18	34.99	34.16
TiO_2	0.12	0.10	0.10	0.11
Al_2O_3	2.14	1.93	2.01	1.94
Met. Fe	1.63	1.06	5.44	0.93
Fe_2O_3	7.85	24.66	11.61	19.73
FeO	12.95	5.58	10.42	7.45
MnO	0.31	0.26	0.25	0.26
CaO	1.70	1.50	1.55	1.43
MgO	23.87	19.98	21.90	21.09
Na_2O	0.84	0.71	0.77	0.58
K_2O	0.10	0.10	0.10	0.07
H_2O	1.85	3.94	2.33	3.06
H_2O	0.26	0.41	0.28	0.45
P_2O_5	0.27	0.33	0.22	0.32
FeS	5.84	3.90	5.13	5.11
Ni Met.	0.37	0.16	0.70	0.19
NiO	1.06	1.53	1.15	1.77
Cr_2O_3	0.53	0.49	0.48	0.48
TOTAL	100.05	99.82	99.43	99.13
Tot. Fe as metal	20.90	25.13	24.92	23.77

4. BIBLIOGRAPHY

Brannock and Berthold, "The Determination of Sodium and Potassium in Silicate Rocks by Flame Photometer, U. S. Geol. Survey Bull. 992, pt. 1, (1953).

Bridgeman, P. W., High pressure effects, in American Institute of Physics Handbook, 1957.

Clark, Sydney, Absorption Spectra of Some Silicates in the Visible and Near Infrared, American Mineralogist, Vol. 42, 1957.

Dollfus, A., Nourelle recherche d'une atmosphere au voisinage de la lune, Comptes rendus, Academie des Sciences, Paris, Vol. 234, pp. 2046-2049, 1952.

Elsmore, B., Radio observations of the lunar atmosphere, Phil. Mag., 2, 1040-1046, 1957.

Hillebrand, Lundell, Bright, and Hoffman, "Applied Inorganic Analysis", 2nd Ed. Wiley, New York, 1953.

Keenan, Philip, The Measurement of Lunar Color Differences, Astronomical Society of the Pacific, Vol. 43, pp. 203-214, 1931.

Kitson and Mellon, "Colorimetric Determinations of Phosphorus as Molybdivanadophosphoric Acid, Eng. Chem., Anal. Ed., 16, 379 (1944).

Kuiper, G. P., Planetary atmospheres and their origin, in The Atmosphere of the Earth and Planets, Revised Edition, (G. P. Kuiper, editor), p. 367, University of Chicago Press, Chicago, 1952.

Launer, Philip, Regularities in the Infrared Absorption Spectra of Silicate Minerals, American Mineralogist, Vol. 37, 1952.

Loeb, L. B., Kinetic Theory of Gases, First Edition, pp. 94-97, McGraw-Hill Book Company, Inc., New York, 1927.

Lundell, Hoffman, Bright, "Chemical Analysis of Iron and Steel", Wiley, New York, 1931, p. 152.

Oke, J. B., Standard Stars for Photoelectric Spectrophotometry, Astrophysical Journal, Vol. 131, No. 2, 1960.

Opik, E. J., and S. F. Singer, Escape of gases from the moon, J. Geophys. Research, 65, 3065-3070, 1960.

Pettit, E., radiation measurements on the eclipsed moon, Astrophys. J. 91, 408, 1940.

Pettit, E., and S. B. Nicholson, Lunar radiation and temperatures, Astrophys. J., 71, 102, 1930.

Riott, "Determining Metallic Iron in Iron Oxides and Slags, Ind. Eng. Chem., Anal. Ed., 13, 546 (1941).

Siegel, K. M., "Estimation of the Physical Constants of the Lunar Surface", University of Michigan Radiation Laboratory, Report 3544-1-F, 1960.

Sinton, Wm., and John Strong, Radiometric Observations of Mars, Astrophysical Journal, Vol. 31, No. 2, pp. 459-469, 1960.

Spitzer, L., Jr., The terrestrial atmosphere above 300 Km, in The Atmosphere of the Earth and Planets, Revised Edition, (G. P. Kuiper, editor), pp. 239-244, University of Chicago Press, Chicago, 1952.

Urey, H. C., The Planets, Their Origin and Development, pp. 17-18, Yale University Press, New Haven, 1952.

Watson, K., B. Murray, Harrison Brown, On the possible presence of ice on the moon, accepted for publication as a Letter to the Editor in the Journal of Geophysical Research, 1961.

Willard and Greathouse, "The Colorimetric Determination of Manganese by Oxidation with Periodate, Am. Chem. Soc. Jour., 39, 2366 (1917).